Post-translational Modifications of Fumarase Regulate its Enzyme Activity and Function in Respiration and the DNA Damage Response

Suqing Wang [1†], Dharanidharan Ramamurthy [1†‡], Jasper Tan [1], Jingyan Liu [1], Joyce Yip [1], Andrea Chua [1], Zhang Yu [1], Teck Kwang Lim [2], Qingsong Lin [2], Ophry Pines [3,4*] and Norbert Lehming [1,4*]

1 - ***Department of Microbiology and Immunology,*** *Cancer Programme at NUSMED, CREATE-NUS-HUJ Programme, Yong Loo Lin School of Medicine, National University of Singapore, Singapore*

2 - ***Department of Biological Sciences,*** *Faculty of Science, National University of Singapore, Singapore*

3 - ***Department of Microbiology and Molecular Genetics,*** *IMRIC, Faculty of Medicine, Hebrew University of Jerusalem, Israel*

4 - ***CREATE-NUS-HUJ Programme and Department of Microbiology and Immunology,*** *Yong Loo Lin School of Medicine, National University of Singapore, Singapore*

Correspondence to Ophry Pines and Norbert Lehming: *ophryp@ekmd.huji.ac.il (O. Pines), micln@nus.edu.sg (N. Lehming)*

https://doi.org/10.1016/j.jmb.2020.09.021

Edited by Titia Sixma

Abstract

The Krebs cycle enzyme fumarase is a dual-targeted protein that is located in the mitochondria and cytoplasm of eukaryotic cells. Besides being involved in the TCA cycle and primary metabolism, fumarase is a tumour suppressor that aids DNA repair in human cells. Using mass spectrometry, we identified modifications in peptides of cytosolic yeast fumarase, some of which were absent when the cells were exposed to DNA damage (using the homing endonuclease system or hydroxyurea). We show that DNA damage increased the enzymatic activity of fumarase, which we hypothesized to be affected by post-translational modifications. Succinylation and ubiquitination of fumarase at lysines 78 and 79, phosphorylation at threonine 122, serine 124 and threonine 126 as well as deamidation at arginine 239 were found to be functionally relevant. Upon homology analysis, these residues were also found to be evolutionally conserved. Serine 128, on the other hand, is not evolutionary conserved and the Fum1S128D phosphorylation mimic was able to aid DNA repair. Our molecular model is that the above modifications inhibit the enzymatic activity of cytosolic fumarase under conditions of no DNA damage induction and when there is less need for the enzyme. Upon genotoxic stress, some fumarase modifications are removed and some enzymes are degraded while unmodified proteins are synthesized. This report is the first to demonstrate how post-translational modifications influence the catalytic and DNA repair functions of fumarase in the cell.

Introduction

Eukaryotic proteins exhibit a phenomenon termed dual localization where specific proteins have identical forms that localize in multiple subcellular compartments.[1] Such proteins appear

† The first two authors contributed equally to the work.

‡ Current address: Medical Biotechnology & Immunotherapy Research Unit, Institute of Infectious Disease and Molecular Medicine, Faculty of Health Sciences, University of Cape Town, Cape Town, South Africa.

to have a high degree of evolutionary conservation.[2] From the budding yeast *Saccharomyces cerevisiae* to humans, fumarase is one such conserved protein that is, more or less, equally distributed between mitochondria and the cytosol. Cellular distribution of this enzyme is determined by different molecular mechanisms; in yeast by protein folding of the precursor during translocation and in human by the presence or absence of a mitochondrial targeting sequence (MTS) on its translation products.[2] In mitochondria, fumarase catalyzes the conversion of fumarate to malate which is an intermediate step in the TCA cycle that generates cellular energy through ATP production.[3,4] An increasing body of work offers insights into an additional nuclear function of cytosolic fumarase. Nuclear recruitment of fumarase was found to occur during DNA double-stranded damage in both yeast and human cells. Inside the nucleus, fumarase converts malate to fumarate, and this enzymatic activity plays a critical role in the DNA damage response.[5–7] Worth mentioning is that fumarate hydratase (FH), the human homologue of yeast fumarase, was identified as a tumour suppressor. Mutations that cause bi-allelic inactivation of the FH gene are associated with a rare genetic condition known as hereditary leiomyomatosis and renal cell carcinoma (HLRCC).[8–11]

Homologous recombination (HR) and non-homologous end joining (NHEJ) are two major mechanisms by which eukaryotic cells respond to double-strand breaks (DSBs). Human FH was found to be phosphorylated by DNA-PK at T236, which improves binding of FH to histone H2A.Z as part of the DNA damage response.[6] T236 is not conserved in yeast Fum1 (Supplementary Alignment 1). Another known human FH kinase is the serine-threonine kinase AMP-activated protein kinase (AMPK), which is an enzyme complex that functions as an energy sensor in higher eukaryotes. AMPK, activated by glucose deficiency, phosphorylates FH at S75.[12] Yeast fumarase, Fum1, was described to become acetylated[13] and succinylated[14] at K58, phosphorylated at T428,[15] and ubiquitinated at K448.[16]

In this study, we aimed to investigate the effects of PTMs on the catalytic activity and on the DNA repair function of fumarase. Using *S. cerevisiae*, we identified and characterized six new functionally relevant PTM sites in the cytosolic fumarase protein. These modifications were detected under normal growth conditions and were absent when DSBs were induced. We found that the PTMs in these evolutionally conserved amino acid residues had an inhibitory effect on the enzymatic activity of fumarase. Our hypothesis is that through these specific PTMs, cells regulate the enzymatic activity of cytosolic fumarase. In response to DNA damage, some of the PTMs are removed and some of the modified enzymes are degraded while the modifications of newly synthesized enzymes are blocked.

Results

The specific enzymatic activity of cytosolic fumarase increases by three-fold upon DNA damage

In this study, we used haploid *BY*4741Δ*W*, *BY*4742Δ*W* and diploid *BY*4743Δ*W* yeast strains as well as their isogenic *FUM1* gene deletion derivatives. Our approach was to express fumarase from either a multi-copy plasmid under the control of the strong constitutive *ACT1* promoter for over-expression or from a single-copy plasmid under the control of its own promoter for expression at endogenous protein levels. *BY*4742Δ*W*Δ*FUM1* cells that had been transformed with the *PactT424-Fum*1Δ*MTS* plasmid expressing cytosolic Fum1ΔMTS from the *ACT1* promoter were grown in glucose media to mid-exponential phase A_{600nm} = 1. The culture was split and one half was allowed to grow for an additional hour (Glu), while the other half was grown for an additional two hours under conditions of DNA damage (400 mM hydroxyurea, HU). Under conditions of DNA damage, the cells divide at half the speed as compared to normal conditions, which means that an equal amount of cells was obtained for both conditions. We performed the maleic enzyme-coupled fumarase enzyme assay with protein extracts isolated from these cells. We found that the specific enzymatic activity of cytosolic fumarase increased approximately three-fold upon DNA damage (Figure 1(a)), while the protein expression of cytosolic fumarase did not change (Figure 1(b)). A cycloheximide (protein translation inhibitor) chase was performed in order to determine if the increase in specific enzymatic activity required the production of new protein (Figure 1(c)). Figure 1 (d) shows that the fumarase enzymatic activity normalized to the total protein concentration decreased during the three hour cycloheximide chase (left bars). In contrast, the fumarase specific enzymatic activity increased when normalized to the amount of cytosolic fumarase as detected by the Western Blot in Figure 1(c) (right bars). This result suggests that the increase was due to differences in post-translational modifications. However, after two hours of DNA damage, the increase in enzymatic activity is higher in the absence of cycloheximide, suggesting that it is also due in part to the production of new protein. The cycloheximide chase experiments also show that cytosolic fumarase is less stable when the cells are grown under conditions of DNA damage (half-life Glu = 7.5 h; half-life HU = 2.8 h; Supplementary

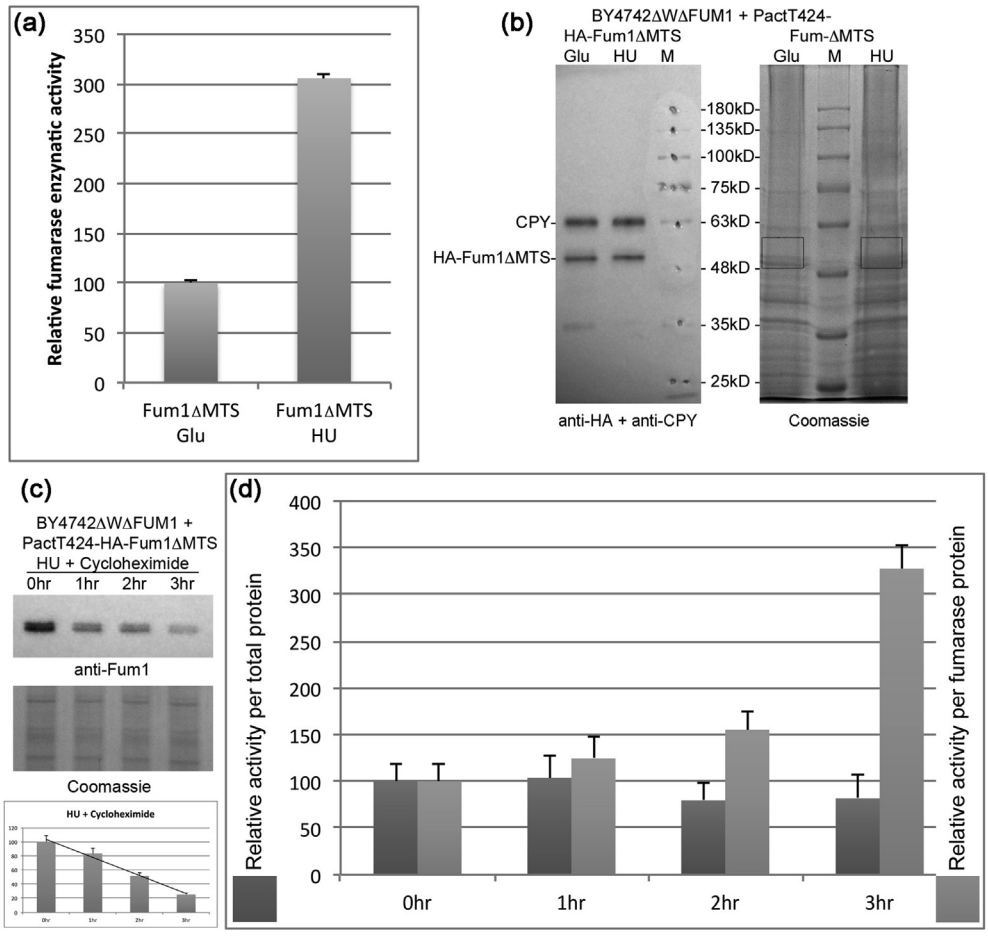

Figure 1. The enzymatic activity of cytosolic fumarase increased by approximately three-fold upon DNA damage. (a) *BY4742ΔWΔFUM1* cells were transformed with the multi-copy vector *PactT424-Fum1ΔMTS* expressing cytosolic fumarase under the control of the *ACT1* promoter/terminator cassette. Cells were grown in liquid glucose media to mid-log phase, after which the cultures were split in half and incubated for one additional hour in liquid glucose media without HU (Glu) or incubated for two additional hours in liquid glucose media containing 400 mM HU (HU). Fumarase activites in the protein extracts were determined by measuring the increase in A_{340nm} over the course of 10 min with the malic enzyme-coupled assay. The activities were normalized to the total protein concentration determined by nano drop. (b) Cells expressing cytosolic HA-Fum1ΔMTS under the depicted conditions were boiled in SDS loading dye, proteins were separated on an 8% PAA gel, transferred to nitrocellulose and HA-Fum1ΔMTS was detected with the help of an anti-HA antibody, while an anti-Carboxypeptidase Y (CPY) antibody served as loading control (left panel). Proteins in the right panel were detected with the help of coomassie and bands corresponding to the size of HA-Fum1ΔMTS were excised as indicated by the boxes, in-gel trypsinated and subjected to MS. (c) Cycloheximide was added to cells expressing cytosolic fumarase under conditions of DNA damage and aliquots were taken every hour for three hours. Equal amounts of cells were boiled in SDS loading dye and loaded onto two gels. Proteins from one gel were transferred to nitrocellulose and HA-Fum1ΔMTS was visualized with the help of an anti-Fum1 antibody, while proteins in the other gel were visualized with Coomassie and served as loading control. (d) Left bars: Fumarase enzymatic activities of the hourly aliquots of the cycloheximide chase presented in (c) were determined as in (a). Right bars: Fumarase enzymatic activities of the hourly aliquots was normalized to the amount of cytosolic fumarase detected in (c).

Figure 1). Based on these results the approach we have taken was to perform mass spectrometry (MS) of cytosolic fumarase purified from yeast cells grown under normal conditions (Glu) and for two hours under conditions of DNA damage (400 mM hydroxyurea, HU). In order to determine post-translational modifications of cytosolic Fum1 that occur upon DNA damage, we first boiled the cells in loading dye. Then purified cytosolic fumarase was excised from bands corresponding in size to Fum1ΔMTS from a Coomassie-stained 8% polyacrylamide (PAA) gel (Figure 1(b), which was followed by mass spectrometry (MS).

Table 1 shows that after two hours of DNA damage, cytosolic fumarase became phosphorylated at S96, T285 and S303,

Table 1 Post-translational modifications found on cytosolic fumarase. MS results of post-translational modifications found on residues of cytosolic fumarase from *BY*4742Δ*W*Δ*FUM1* yeast cells transformed with the *PactT424-Fum*1Δ*MTS* plasmid grown in either glucose media to mid-log phase A_{600nm} = 1 or for an additional two hours in glucose media containing 400 mM HU. Cells were boiled in SDS loading dye, proteins were separated on an 8% PAA gel and visualized with Coomassie. Bands corresponding to the size of Fum1ΔMTS were in-gel trypsinated. The numbers in brackets indicate the number of peptides with these modification observed by MS.

Residue	Glucose	HU
S96	–	ESLGGLDPKI**Sp**KAIQQAADEVASGK (2)
T285	–	FQ**Tp**APNKFEALAAHDAIVECSGALNTLACSLFK (1)
S303	–	FQTAPNKFEALAAHDAIVEC**Sp**GALNTLACSLFK (1)
K78/K79	PLVHAFGVL**KsuccKub** (12)	PLVHAFGVL**KsuccKub** (1)
K78/K79	PLVHAFGVL**KubKsucc** (11)	–
T122	LDDHFPLVVFQ**Tp**GSGTQSNMNANEVISNR (1)	–
S124	LDDHFPLVVFQTG**Sp**GTQSNMNANEVISNR (2)	–
T126	LDDHFPLVVFQTGSG**Tp**QSNMNANEVISNR (2)	–
S128	LDDHFPLVVFQTGSGTQ**Sp**NMNANEVISNR (2)	–
R239/K245/K264	THLQDATPLTLGQEFSGYVQQVENGIQ **Rdeamidated**VAHSL**Ksucc**TLSFLAQGGTAVGTGLNT**Ksucc**PG (1)	–
K245/K264	THLQDATPLTLGQEFSGYVQQVENGIQRVAHSL **Ksucc**TLSFLAQGGTAVGTGLNT**Ksucc**PG (5)	–
K429	T**Ksucc**SLMLVTALNPK (1)	–

de-phosphorylated at T122, S124, T126 and S128, de-amidated at R239, mostly de-succinylated and de-ubiquitinated at K78 and K79, and de-succinylated at K245, K264 and K429. K78 and K79 were always found to be doubly modified with one lysine succinylated and the other lysine ubiquitinated, while single modifications were not observed. T122, S124, T126 and S128 were found to be singly phosphorylated while doubly modified peptides were not observed. K245 and K264 were always found to be doubly succinylated and single modifications were not observed. R239 was found to be de-amidated on the same peptide together with double-succinylated K245 and K264. T285 and S303 were found to be singly modified and doubly modified peptides were not observed. For modifications that are not located on the same peptide, it is not possible to say if they occur on the same molecule. For those modifications which were observed on one or two peptides only, it is possible that they would have been found under both conditions if more peptides would have been collected.

Phosphorylation of Fum1 at S96, T285, S303 and T428 is not required for the TCA cycle and DNA repair

For the sake of clarity, we present in this and the next sections the analysis of different groups of modifications. In order to determine if phosphorylation of S96, T285 and S303 were required for Fum1 to function in the TCA cycle or to aid DNA repair, we mutated these residues to alanine, which cannot be phosphorylated. Figure 2(a) shows that diploid *BY*4743Δ*W* cells, but not *BY*4743Δ*W*Δ*FUM1* cells, were able to grow on glycerol plates (as a sole carbon and energy source, requiring respiration) and on glucose plates containing 400 mM HU (compare rows 1 and 2), reflecting that Fum1 is required for the utilization of respiration-requiring substrates via the TCA cycle and for the repair of damaged DNA. Figure 2(a), line 4, further shows that wild-type Fum1 C-terminally fused to three HA epitopes and ten histidines and expressed from the single-copy plasmid *YCplac33* under the control of its own promoter (*FUM1-HA*$_3$-*H*$_{10}$-*33*) was able to complement the *FUM1* gene deletion and to support growth on both the glycerol plates and on the glucose plates containing 400 mM HU. Similar results were obtained when cytosolic Fum1 lacking the MTS was expressed from the same plasmid under the control of its own promoter (row 3). Phosphorylation of S96, T285, S303 and also T428 are not required for the function of Fum1 in the TCA cycle and in DNA repair, as mutant proteins changing these residues to alanines were able to support growth on both the glycerol plate and on the plate containing 400 mM HU (compare lines 5 to 12). Alignment 1 shows that while T285 and S303 are conserved between yeast and human, S96 and T428 are not (see also Supplementary Alignment 2). Figure 2(b) shows that all mutant proteins were expressed at protein levels comparable to that of wild-type Fum1.

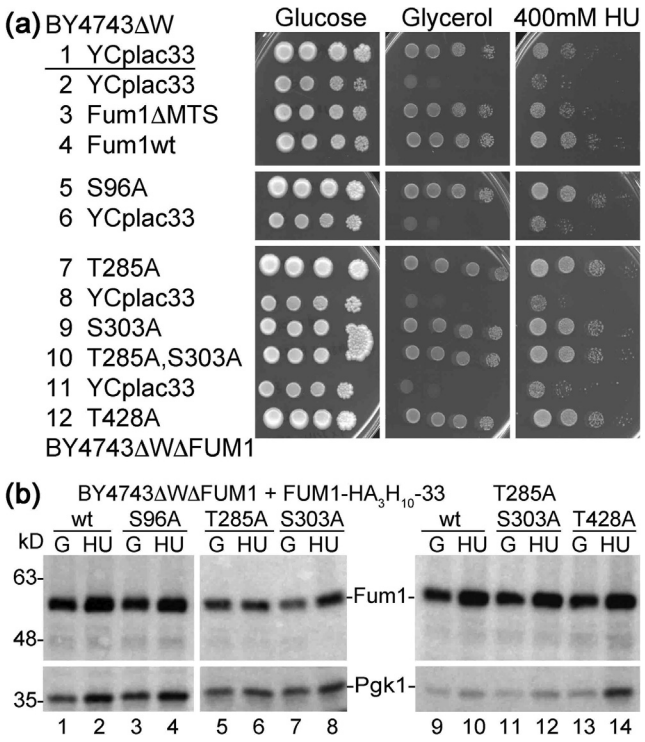

Figure 2. Phosphorylation of Fum1 at S96, T285, S303 and T428 was not required for its functions in TCA cycle and DNA repair. (a) Cells of the indicated genotype expressing the Fum1 derivatives from the single-copy vector *YCplac33* under the control of the *FUM1* promoter were ten-fold serially diluted, spotted onto the depicted plates and incubated for six days at 28 °C. All panels were excised from the plates shown in Supplementary Figure 2. (b) Cells from (a) were grown in glucose liquid media to mid-log phase (G) or incubated for an additional two hours in liquid media containing 400 mM HU (H) and boiled in SDS loading dye. Proteins were separated on 8% PAA gels and transferred to nitrocellulose membranes. Fum1 derivatives were detected with the help of an anti-HA antibody, while an anti-Pgk1 antibody served as the loading control. All panels were excised from the blots shown in Supplementary Figure 3.

```
FH    LDPKIANAI.....FVTAPNKFEALAAHDALVELSGAMNT.....LMNESLMLVTALN
      LDPKI+ AI.....F TAPNKFEALAAHDA+VE SGA+NT.....L+ +SLMLVTALN
Fum1  LDPKISKAI.....FQTAPNKFEALAAHDAIVECSGALNT.....LLTKSLMLVTALN
            96      285                  303        428
```

Alignment 1. Protein sequence alignment between human (FH) and yeast fumarase (Fum1) for the regions around Fum1S96, T285, S303 and T428. The alignment shows that while T285 and S303 are conserved, S96 and T428 are not. The entire alignment between FH and Fum1 is shown as Supplementary Alignment 1. A multiple sequence alignment for fumarase sequences from ten different species (Supplementary Alignment 2) shows that only T285 is completely conserved from yeast to human.

Succinylation of Fum1 at K245, K264 and K429 is not required for the TCA cycle and the DNA repair functions

We asked if succinylation of Fum1 at K245, K264 and K429 affects its function in the TCA cycle and in DNA repair. Figure 3(a) shows that mimicking succinylation by mutating these lysines to glutamic acids or preventing succinylation by mutating these lysines to arginines still supported growth of *BY4743ΔWΔFUM1* cells on glycerol plates and on glucose plates containing 400 mM HU (lines 5–13), demonstrating that the de-succinylation of these lysines was not functionally required. Consistent with our results, the respective lysine residues are not conserved, implying that they may not be important for the appropriate functions (Alignment 2). Figure 3(b) shows that all these variant proteins were expressed at levels comparable to the level of Fum1 wild-type protein.

Unmodified Fum1T122, S124, T126 and R239 are required for Fum1 function in the TCA cycle and DNA repair

Intriguingly, Figure 4(a), indicates that the function of Fum1 in the TCA cycle and in DNA repair was inhibited by the phosphorylation of Fum1 at T122, S124, and T126 and by the

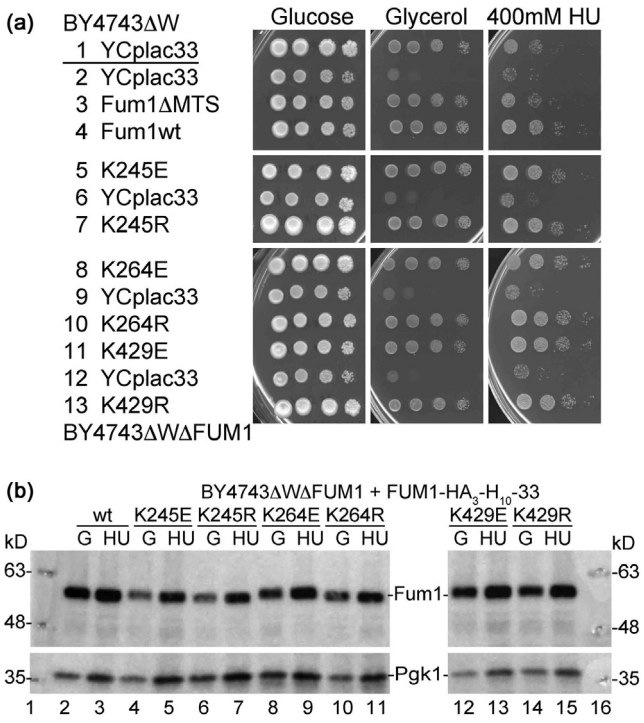

Figure 3. Succinylation of Fum1 at K245, K264 and K429 was not required for its functions in TCA cycle and DNA repair. (a) Cells of the indicated genotype expressing the Fum1 derivatives from the single-copy vector *YCplac33* under the control of the *FUM1* promoter were ten-fold serially diluted, spotted onto the depicted plates and incubated for six days at 28 °C. All panels were excised from the plates shown in Supplementary Figure 2. (b) Cells from (a) were grown in glucose liquid media to mid-log phase (G) or incubated for an additional two hours in liquid media containing 400 mM HU (H) and boiled in SDS loading dye. Proteins were separated on 8% PAA gels and transferred to nitrocellulose membranes. Fum1 derivatives were detected with the help of an anti-HA antibody, while an anti-Pgk1 antibody served as the loading control. All panels were excised from the blots shown in Supplementary Figure 3.

```
FH    261 RIKAAMPRIYELAAGGTAVGTGLNTRIGF.....LMNESLMLVTALNP
          R+   ++   +   LA GGTAVGTGLNT+ GF.....L+ +SLMLVTALNP
Fum1  239 RVAHSLKTLSFLAQGGTAVGTGLNTKPGF.....LLTKSLMLVTALNP
                245                    264       429
```

Alignment 2. Protein sequence alignment between human (FH) and yeast fumarase (Fum1) for the regions around Fum1K245, K264 and K429. The alignment shows that all three lysines are not conserved between yeast and human.

deamidation of Fum1 at R239. Cells expressing the Fum1T122E, S124D, T126E and R239Q modification mimics failed to grow on glycerol plates and on on glucose plates containing 400 mM HU. As a control we show that cells expressing the catalytically inactive Fum1H154R mutant protein, similarly, do not grow under these conditions (rows 3–15). It is important to stress that these modifications of cytosolic Fum1, which had been observed in cells grown under normal conditions, were absent after two hours of growth under conditions of DNA damage (Table 1). While each of these individual modifications were observed on one or two peptides only, as a group, these inactivating modifications were observed on six peptides when the cells had been grown under normal conditions and not at all when the cells had been grown under conditions of DNA damage. Our results indicate that cytosolic Fum1 is inhibited by the post-translational modifications on these residues, when cells are grown under normal conditions, and presumably when cytosolic Fum1 activity is less required. Upon DNA damage, cytosolic Fum1 may be activated by removal of these modifications on the specific residues or by the degradation of the modified Fum1 proteins and synthesis of unmodified Fum1 molecules. The only exception in this group is S128, as cells expressing the Fum1S128D mutant protein were still able to grow on the glycerol plate

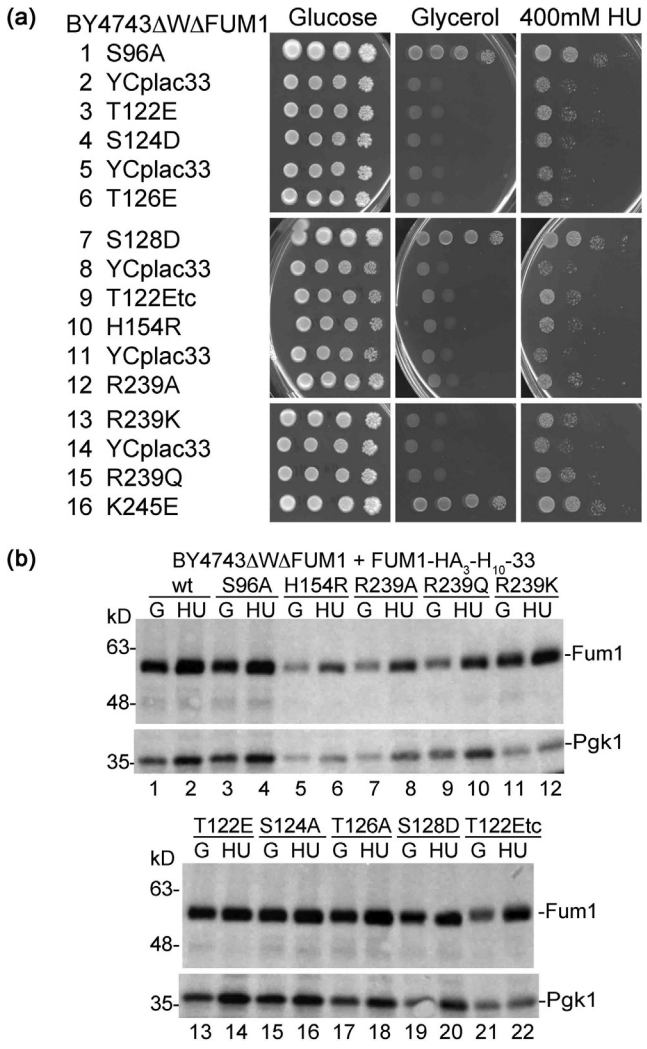

Figure 4. Phosphorylation of Fum1 at T122, S124 and T126 and deamidation of R239 inhibited its functions in TCA cycle and DNA repair, while phosphorylation of Fum1 at S128 did not. (a) Cells of the indicated genotype expressing the Fum1 derivatives from the single-copy vector *YCplac33* under the control of the *FUM1* promoter were ten-fold serially diluted, spotted onto the depicted plates and incubated for six days at 28 °C. All panels were excised from the plates shown in Supplementary Figure 2. (b) Cells from (a) were grown in glucose liquid media to mid-log phase (G) or incubated for an additional two hours in liquid media containing 400 mM HU (H) and boiled in SDS loading dye. Proteins were separated on 8% PAA gels and transferred to nitrocellulose membranes. Fum1 derivatives were detected with the help of an anti-HA antibody, while an anti-Pgk1 antibody served as the loading control. All panels were excised from the blots shown in Supplementary Figure 3.

```
FH    134 DHFPLVVWQTGSGTQTNMN.....VHPN.....GQEFSGYVQQVKYAMTR 261
          DHFPLVV+QTGSGTQ+NMN.....VHPN.....GQEFSGYVQQV+   + R
Fum1  110 DHFPLVVFQTGSGTQSNMN.....VHPN.....GQEFSGYVQQVENGIQR 239
                  122-126 128    154
```

Alignment 3. Protein sequence alignment between human (FH) and yeast fumarase (Fum1) for the regions around Fum1T122, S124, T126, S128, H154 and R239. The alignment shows that while T122, S124, T126, H154 and R239 are conserved between yeast and human, S128 is not. A multiple sequence alignment for fumarase sequences from ten different species (Supplementary Alignment 2) shows that T122, S124, T126, H154 and R239 are completely conserved from yeast to human.

and on the glucose plate containing HU (row 7). Consistently, T122, S124, T126, H154 and R239 are conserved from yeast to human, while S128 is not (Alignment 3 and Supplementary Alignment 2). Similar results were obtained for haploid *BY*4741Δ*W* cells expressing the same modification mimics (Supplementary Figure 5). Figure 4(b) shows that all Fum1 variant proteins were expressed at levels comparable to the levels of the wild-type proteins.

The Fum1 modification mimics T122E, S124D, T126E, S128D and R239Q showed decreased enzymatic activity as compared to wild-type Fum1

Figure 5 shows that the fumarase enzyme assay performed with protein extracts derived from *BY*4743Δ*W*Δ*FUM1* yeast cells expressing Fum1-HA_3-H_{10} from the single-copy vector *YCplac33* under the control of its own promoter increased approximately three-fold when the cells had been exposed to conditions of DNA damage for two hours. The figure further shows that protein extracts derived from cells expressing the Fum1 mutant proteins T122E, S124D, T126E, S128D and H154R displayed lower levels of fumarase enzyme activity. The S128D mutant, which had been able to grow on glycerol plates and on plates containing 400 mM HU, generated the highest enzymatic activity compared to the other mutant proteins. However, this enzyme activity was still lower than wild-type fumarase in cells grown under normal conditions.

Succinylation/ubiquitination of Fum1 at K78 and K79 inhibits its functional roles in the TCA cycle and DNA repair

Figure 6(a) shows that succinylation of K78 and K79 affected the functions of Fum1 in the TCA cycle and in DNA repair, as cells expressing the succinylation mimics K78E (row 8), K79E (row 11) and K78E/K79E (K789E; row 5) were unable to grow on the glycerol plates and on the plates containing 400 mM HU. The figure further shows mutants in which both lysines were changed simultaneously to either alanine, which takes away the positive charges of the lysines (K789A; row 4), or arginine, which maintains the positive charges of the lysines and prevents succinylation and ubiquitination (K789R; line 6). These Fum1 mutant proteins were unable to support TCA cycle and DNA repair. On the other hand, changing just K79 to arginine resulted in a Fum1 mutant protein that was able to support both functions (row 12). The Fum1K78A mutant protein was unable to support TCA cycle and DNA repair (row 7), while the K78R (row 9) and K79A (row 10) mutant proteins were able to support the TCA cycle but not DNA repair. These results indicate that unmodified K78 is more important for fumarase function than K79. Consistently, K78 is conserved from yeast to human, while K79 is conserved from yeast to fish only, and an arginine can be found in this position from bird to human (Alignment 4 and Supplementary Alignment 2).

Figure 6(b) shows that the Fum1K78/K79 double mutant proteins are expressed at much lower levels as compared to the one of the Fum1 wild-type

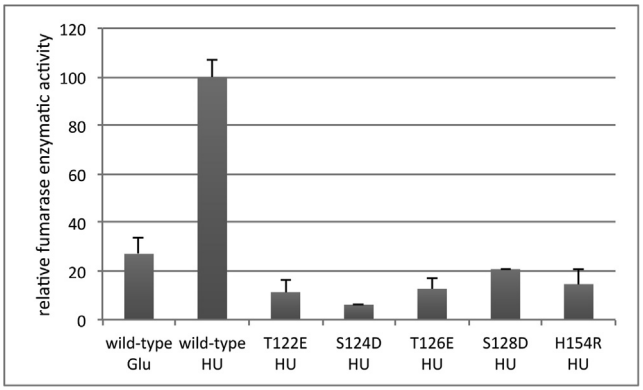

Figure 5. The specific enzymatic activity of wild-type fumarase increased by approximately three-fold upon two hours of DNA damage, while the specific enzymatic activities of the fumarase mutant proteins T122E, S124D, T126E, S128D and H154R remained low. *BY*4743Δ*W*Δ*FUM1* yeast cells expressing the Fum1-HA_3-H_{10} wild-type and mutant proteins from the single-copy vector *YCplac33* under the control of the *FUM1* promoter were grown in glucose liquid media to mid-log phase (Glu) or incubated in liquid media containing 400 mM HU for another two hours (HU). Protein extracts were obtained by bead beating and the maleic enzyme-coupled fumarase enzyme assay was performed by measuring the increase in A_{340nm} over a time course of 10 min. Error bars indicate the standard deviation of assays performed in triplicates, where averages had been normalized to the total protein concentrations and to the signals of the respective Fum1 mutant proteins in the Western Blots shown in Figure 4.

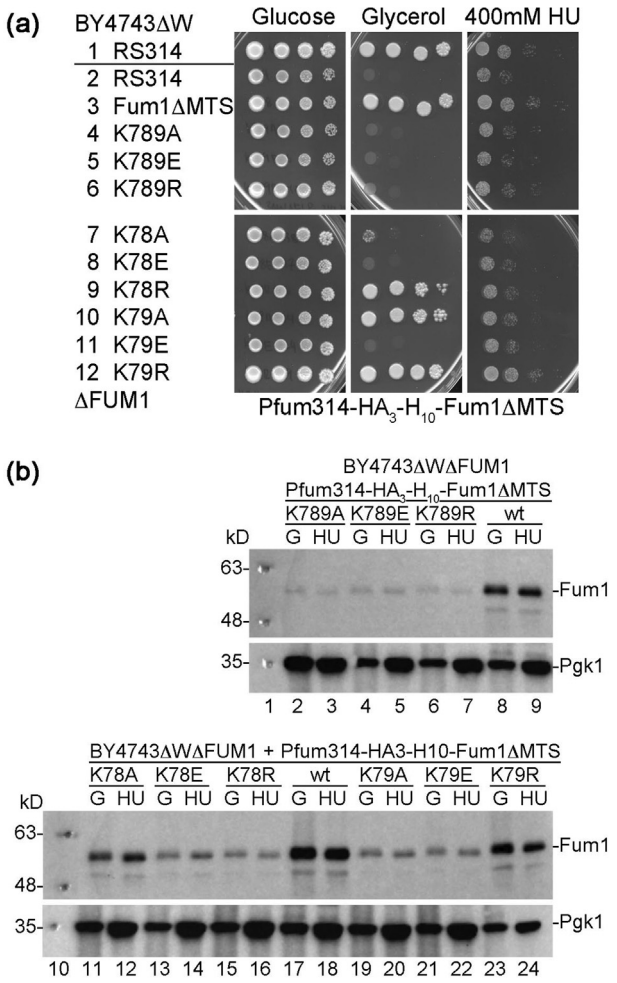

Figure 6. Succinylation of Fum1 at K78 and at K79 inhibited its functions in TCA cycle and DNA repair. (a) Cells of the indicated genotype expressing the cytosolic HA_3-H_{10}-Fum1ΔMTS derivatives from the single-copy vector *RS314* under the control of the *FUM1* promoter were ten-fold serially diluted, spotted onto the depicted plates and incubated for six days at 28 °C. All panels were excised from the plates shown in Supplementary Figure 4. (b) Cells from (a) were grown in glucose liquid media to mid-log phase (G) or incubated for an additional two hours in liquid media containing 400 mM HU (H) and boiled in SDS loading dye. Proteins were separated on 8% PAA gels and transferred to nitrocellulose membranes. Fum1 derivatives were detected with the help of an anti-HA antibody, while an anti-Pgk1 antibody served as the loading control.

```
FH    77 NFKIGGVTERMPTPVIKAFGILKRAAAEVNQDYG-LDPKIANAI 121
         NFKIGG  ERMP P++ AFG+LK++AA VN+  G LDPKI+ AI
Fum1  55 NFKIGGARERMPLPLVHAFGVLKKSAAIVNESLGGLDPKISKAI  99
                              K78/K79
```

Alignment 4. Protein sequence alignment between human (FH) and yeast fumarase (Fum1) for the region around Fum1K78 and K79. The alignment shows that while K78 is conserved between yeast and human, K79 is not. Supplementary Alignment 2 shows that K78 is completely conserved from yeast to human, while K79 is conserved from yeast to fish and an arginine can be found in this position from bird to human.

protein (lanes 2–9). A likely explanation for these low expression levels is their degradation. The low expression levels could explain why cells expressing these three double mutant proteins were unable to grow on glycerol plates and on glucose plates containing 400 mM HU. Worth mentioning is that the Fum1K78 and Fum1K79 single mutant proteins were expressed at levels higher than the double mutant proteins but lower than the Fum1 wild-type protein (rows 11–24). The Fum1K79A protein, which supported TCA cycle but not DNA repair, was expressed at lower

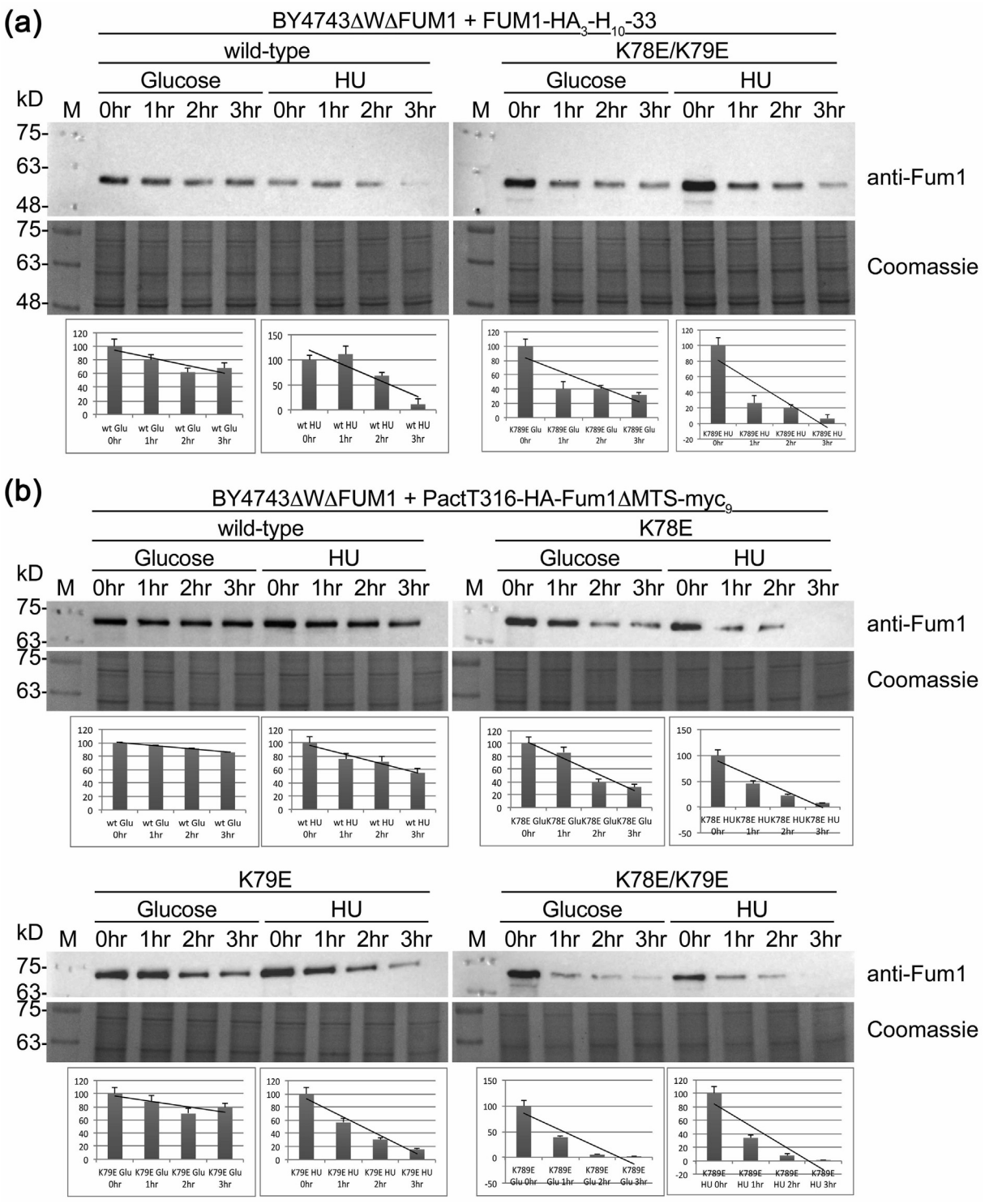
(a)
BY4743ΔWΔFUM1 + FUM1-HA3-H10-33
wild-type
K78E/K79E
Glucose
HU
kD
M
0hr 1hr 2hr 3hr 0hr 1hr 2hr 3hr
M 0hr 1hr 2hr 3hr 0hr 1hr 2hr 3hr
75-
63-
48-
anti-Fum1
Coomassie
wt Glu 0hr
wt Glu 1hr
wt Glu 2hr
wt Glu 3hr
wt HU 0hr
wt HU 1hr
wt HU 2hr
wt HU 3hr
K789E Glu 0hr
K789E Glu 1hr
K789E Glu 2hr
K789E Glu 3hr
K789E HU 0hr
K789E HU 1hr
K789E HU 2hr
K789E HU 3hr
(b)
BY4743ΔWΔFUM1 + PactT316-HA-Fum1ΔMTS-myc9
wild-type
K78E
K79E
K78E/K79E
anti-Fum1
Coomassie
K78E Glu 0hr
K78E Glu 1hr
K78E Glu 2hr
K78E Glu 3hr
K78E HU 0hr
K78E HU 1hr
K78E HU 2hr
K78E HU 3hr
K79E Glu 0hr
K79E Glu 1hr
K79E Glu 2hr
K79E Glu 3hr
K79E HU 0hr
K79E HU 1hr
K79E HU 2hr
K79E HU 3hr
K789E Glu 0hr
K789E Glu 1hr
K789E Glu 2hr
K789E Glu 3hr
K789E HU 0hr
K789E HU 1hr
K789E HU 2hr
K789E HU 3hr

protein levels as compared to the Fum1K79R protein, which supported both functions, and the difference in fumarase protein levels could explain the difference in phenotypes. We performed cycloheximide chase assays to compare the protein stability of wild-type fumarase with the three succinylation mimics K78E, K79E and K78E/K79E. Figure 7(a) shows that the full-length double succinylation mimic Fum1K78E/K79E expressed from a single-copy vector under the control of the *FUM1* promoter was less stable than wild-type Fum1 expressed from the same plasmid under both normal conditions and under conditions of DNA damage. Figure 7(b) shows that cytosolic wild-type Fum1 expressed from the *ACT1* promoter and fused to nine myc epitopes was more stable than the three succinylation mimics K78E, K79E and K78E/K79E expressed from the same plasmid under both normal conditions and under conditions of DNA damage. In order to further study the contribution of the low fumarase protein expression on the phenotype, we expressed the three cytosolic HA-Fum1ΔMTS succinylation mimics K78E, K79E and K78E/K79E fused to nine myc epitopes from the strong *ACT1* promoter. Figure 8(b) shows that all three succinylation mimics are expressed at protein levels higher than that of wild-type cytosolic HA_2-Fum1ΔMTS from its own promoter (compare lanes 2 and 3 with lanes 6–11). Figure 8(a) shows that the K79E succinylation mimic weakly supports growth on the glycerol plate (compare lines 7 and 8 with lines 9 and 10), while the K78E and the K78E/K79E succinylation mimics fail to do so (compare lines 3 and 4 with lines 5 and 6, as well as lines 9 and 10 with lines 11 and 12). The result confirms our hypothesis that the fully conserved residue K78 is essential for enzyme function, while the less conserved residue K79 is less important.

Recruitment of Fum1 to the site of DNA damage is not a requirement for it to aid DNA repair

Previous studies showed that human FH is recruited to the site of damaged DNA.[6,12] In order to test if Fum1 is recruited, we set up the HO system in *BY*4742Δ*W* and *BY*4742Δ*W*Δ*FUM1* cells. Cleavage of the *HO*-site by the HO endonuclease is required for mating-type switching in *S. cerevisiae*. The original *HO*-site in *BY*4742Δ*W* and *BY*4742Δ*W*Δ*FUM1* cells carry the stuck-mutation,[17] which is not cleaved efficiently, and the HO endonuclease carries four mutations, which render it unable to cleave the *HO*-site.[18] We knocked in a consensus *HO*-site between the *HIS3* and *DED1* loci and expressed HO from the *TRP1*-marked plasmid *HOT1* under the control of the inducible *GAL10* promoter.[19] Figure 9(a) shows that the cells that had been transformed with the

Figure 7. The Fum1 succinylation mimics K78E, K79E and K78E/K79E are less stable than wild-type Fum1. (a) *BY*4743Δ*W*Δ*FUM1* cells expressing full-length wild-type Fum1 or the K78E/K79E double succinylation mimic fused to three HA epitopes and ten histidines from a single-copy vector under the control of its own promoter were grown to mid-log phase. Cycloheximide was added and half of the cultures were incubated in the absence of DNA damage (Glucose), while the other half of the cultures were incubated in the presence of DNA damage (HU). Aliquots were taken each hour for three hours. Equal amounts of cells were boiled in SDS loading dye and proteins were separated on two sets of polyacrylamide gels. The proteins from one set were transferred to nitrocellulose membranes and Fum1 was visualized with an anti-HA antibody, while the proteins in the other set were visualized with Coomassie and served as loading controls. The excel function trendline was used to calculate the half-life of wild-type full-length fumarase in cells grown under normal conditions as 5 h and in cells grown under conditions of DNA damage as 3 h, while the half-life of the full-length Fum1K78E/K79E double succinylation mimic was 2.5 h in cells grown under normal conditions and 2 h in cells grown under conditions of DNA damage. (b) *BY*4743Δ*W*Δ*FUM1* cells expressing cytosolic wild-type Fum1ΔMTS or the succinylation mimics K78E, K79E and K78E/K79E fused to nine myc epitopes from a single-copy vector under the control of the *ACT1* promoter were grown to mid-log phase. Cycloheximide was added and half of the cultures were incubated in the absence of DNA damage (Glucose), while the other half of the cultures were incubated in the presence of DNA damage (HU). Aliquots were taken each hour for three hours. Equal amounts of cells were boiled in SDS loading dye and proteins were separated on two sets of polyacrylamide gels. The proteins from one set were transferred to nitrocellulose membranes and Fum1 was visualized with an anti-myc antibody, while the proteins in the other set were visualized with Coomassie and served as loading controls. The excel function trendline was used to calculate the half-life of wild-type cytosolic fumarase in cells grown under normal conditions as 11.7 h and in cells grown under conditions of DNA damage as 4.4 h, while the half-life of the cytosolic Fum1K78E succinylation mimic was 3 h in cells grown under normal conditions and 2.3 h in cells grown under conditions of DNA damage and the half-life of the Fum1K79E succinylation mimic was 6.6 h in cells grown under normal conditions and 2.5 h in cells grown under conditions of DNA damage and the half-life of the cytosolic Fum1K78E/K79E double succinylation mimic was 2.1 h in cells grown under normal conditions and 2 h in cells grown under conditions of DNA damage. The full gel pictures can be seen under Supplementary Figure 6.

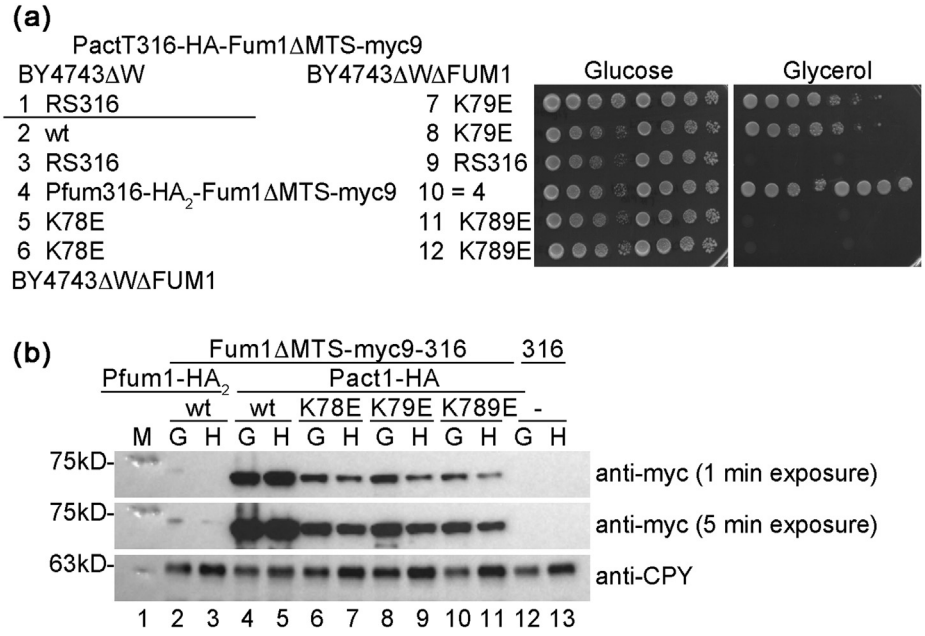

Figure 8. Upon over-expression, the succinylation mimic Fum1K79E was able to support the TCA cycle, while the succinylation mimic Fum1K78E failed to do so. (a) *BY*4743Δ*W*Δ*FUM1* cells expressing the cytosolic HA-Fum1ΔMTS-myc9 derivatives from the single-copy vector *RS316* under the control of the strong *ACT1* promoter were ten-fold serially diluted, spotted onto the depicted plates and incubated for six days at 28 °C. Line 1 contains *BY*4743Δ*W* cells with the empty vector *RS316* and lines 2–12 contain *BY*4743Δ*W*Δ*FUM1* cells. Cells in lines 4 and 10 express wild-type HA_2-Fum1ΔMTS-myc9 from the single-copy vector *RS316* under the control of the *FUM1* promoter, while cells in line 3 contains RS316. Cells in all other lines express the indicated HA-Fum1ΔMTS-myc9 derivatives from the single-copy vector *RS316* under the control of the strong *ACT1* promoter. (b) Cells from (a) were grown in glucose liquid media to mid-log phase (G) or incubated for an additional two hours in liquid media containing 400 mM HU (H) and boiled in SDS loading dye. Proteins were separated on 8% PAA gels and transferred to nitrocellulose membranes. Fum1 derivatives were detected with the help of an anti-myc antibody, while an anti-CPY antibody served as the loading control.

empty *TRP1*-marked vector *YCplac22* (22) were able to grow on both glucose and galactose plates lacking tryptophan (row 1 and 3). The figure further shows that the cells that had been transformed with the *HOT1* plasmid grew on the glucose plate lacking tryptophan, but not on the galactose plate lacking tryptophan (rows 2 and 4), suggesting that the cells died upon cleavage of the *HO*-site. Next, we performed chromatin immunoprecipitation (ChIP) by transforming *BY*4742Δ*W*Δ*FUM1* cells with the single-copy plasmids expressing Fum1-HA_3-H_{10} under the control of its own promoter. Following galactose induction for two hours, proteins were cross-linked to DNA and Fum1-HA_3-H_{10} was precipitated with anti-HA antibody-coupled beads. The amount of Fum1 recruited to the *HO*-site was determined with qPCR primers next to the *HO*-site. Figure 9(b) shows that recruitment of Fum1 wild-type protein increased by approximately five-fold upon cleavage of the *HO*-site when galactose-induced cells were transformed with the *HOT1* plasmid compared to empty vector *YCplac22* control. The figure further shows that the Fum1 mutant proteins K78E/K79E (K789E), T122E, S124D, T126E, S128D, H154R and R239Q were not recruited to the cleaved *HO*-site. Notably, Fum1S128D mutant protein was not recruited to the site of DNA damage, suggesting that the mutation S128D in fumarase prevents the recruitment of fumarase to the site of DNA damage. However, Figure 4(a) demonstrates that Fum1S128D was still able to support both TCA cycle and DNA repair. This suggests that the recruitment of Fum1 to the site of damaged DNA may not be a requirement for its functional role in DNA damage response and repair.

Discussion

Repairing double stranded lesions in DNA is a fundamental cellular process that ensures faithful gene expression, regulation and transmission of intact genetic information to subsequent generations of dividing cells.[20] Defects in the double-stranded repair machinery leads to compromised immunity, tumorigenesis and cell death.[21] Homologous recombination (HR) and non-homologous end joining (NHEJ) are two major mechanisms by which eukaryotic cells respond to double-strand breaks (DSBs).[22,23]

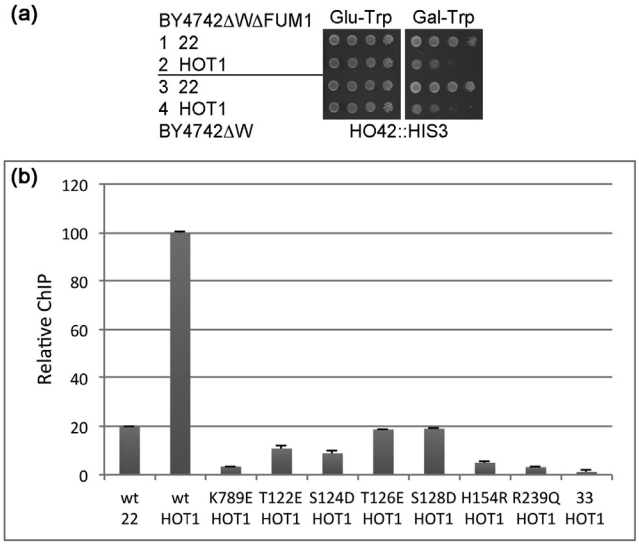

Figure 9. Recruitment of Fum1 to the site of DNA damage was not a requirement to aid DNA repair. (a) A consensus *HO*-site was knocked in between the *HIS3* and *DED1* loci on yeast chromosome 15 of the *BY4742ΔWΔFUM1* yeast (*HO42::HIS3*). Cells transformed with the *TRP1*-marked empty vector control *YCplac22* (22) or with the *TRP1*-marked vector expressing the HO endonuclease under the control of the *GAL10* promoter (*HOT1*) were ten-fold serially diluted, spotted onto the depicted plates and incubated for three days at 28 °C. (b) *BY4742ΔWΔFUM1 HO42::HIS3 +22* and *BY4742ΔWΔFUM1 HO42::HIS3+HOT1* cells were transformed with the single-copy *FUM1-HA*$_3$*-H*$_{10}$*-33* plasmids expressing wild-type Fum1 or the indicated Fum1 mutant proteins from the *FUM1* promoter or with the empty vector *YCplac33* (33). Cells were grown in raffinose liquid media to mid-log phase and incubated for another two hours in galactose liquid media. Proteins were crosslinked to DNA with formaldehyde and chromatin extracts were prepared by bead beating zymolase treated cells. Fum1-HA$_3$-H$_{10}$ crosslinked to DNA was precipitated with HA-coupled beads and the amount of co-precipitated DNA relative to input DNA and Fum1 wild-type protein with *HOT1* was measured by qPCR with primers next to the *HO*-site. The error bars indicate the standard deviations between quadruplets. For simplicity, the figure contains the results for the empty vector *YCplac22* (22) control for wild-type Fum1 only. The entire set with empty vector controls for all mutant Fum1 proteins can be found as Supplementary Figure 7.

The enzyme fumarase (FH) is a celebrated example of a metabolic enzyme that is involved in the DNA damage response in human, yeast and bacteria.[4] As mentioned in the Introduction, fumarase has been shown to undergo post-translational modifications. In human cells, FH was found to be phosphorylated by DNA-PK at T236, which improves binding of FH to histone H2A.Z, and fumarate produced by phosphorylated FH promotes NHEJ through recruitment of DNA-PK at DSB regions. An effect of the phosphorylation of FH at T236 by DNA-PK on the catalytic activity of FH has not been reported[11] and it is important to state that T236 is not conserved in yeast Fum1 (Supplementary Alignments 1 and 2). Another known FH kinase is the serine-threonine kinase AMP-activated protein kinase (AMPK), which is an enzyme complex that functions as an energy sensor in higher eukaryotes. It was reported that AMPK, activated by glucose deficiency, phosphorylates FH at S75. This promotes its binding to the transcription factor ATF2, which affects cell growth.[12] Upon binding to ATF2, FH is recruited to the ATF2 target promoters, where it generates fumarate, which inhibits the H3K36me2 demethylase KDM2A. Notably, there was no reported change in the enzymatic activity of FH and mutating S75 to D, to mimic phosphorylation, did not change the enzymatic activity of FH.[12] Homology analysis revealed that this residue is conserved throughout the fumarases of model organisms investigated. Thus, post-translational modification of human fumarase in the above examples has functional manifestations but no known effect on fumarase enzyme activity.

Yeast fumarase, Fum1, was described to become acetylated[13] and succinylated[14] at K58, phosphorylated at T428,[15] and ubiquitinated at K448.[16] However, all these modifications were identified in proteomic screens with yeast cells grown under a single condition, and no functional relevance was established. In this study we have detected a series of modifications on yeast fumarase derived peptides. Nevertheless, none of previously reported modifications were detected. Thus, overexpression of Fum1 allowed the detection of PTMs in Fum1, yet it is unlikely that the modifications we have listed are exhaustive.

As pointed out, for the sake of clarity we divided the analysis into groups. The approach was straight forward; if changing the respective amino acids by mutagenesis had an effect on TCA cycle

and/or DNA damage phenotypes we concluded that the modifications have a significant effect on protein activity and function. For the first two groups of fumarase modifications described, in fact, we did not find support for their importance for fumarase function in the TCA cycle or DNA repair. Group 1 (S96, T285, S303 and T428) includes amino acids which are phosphorylated upon DNA damage, yet their substitution has no apparent effect on TCA cycle or DNA repair. The same is true for group 2 (K245, K264 and K429) in which we find that mimicking succinylation (by mutating these lysines to glutamic acids) or preventing succinylation (by mutating these lysines to arginines) still supported TCA cycle and DNA repair related functions. With this stated we cannot rule out the participation of these amino acids in combination with other parts of the Fum1 protein or their contribution only under specific physiological conditions.

Group 3 includes removal of phosphorylation on Fum1 at T122, S124, and T126 following DNA damage induction. Consistently, T122, S124 and T126 are conserved from yeast to human, again suggesting significance of these residues. It is important to stress that these modifications of cytosolic Fum1, observed in cells grown under normal conditions, were absent following induction of DNA damage. Furthermore, corresponding Fum1 mutant proteins (e.g. mimics) were expressed at levels comparable to the levels of the wild-type proteins. Based on these finding we hypothesise that under conditions of DNA damage, fumarase undergoes de-phosphorylation and this is an element of the DNA damage response in yeast. Worth mentioning is that unmodified Fum1R239 is also required for the increase in fumarase activity upon DNA damage much like the removal of phosphorylation in Fum1T122, S124 and T126 described above. The only exception in this group is S128, as cells expressing the Fum1S128D mutant protein were still able to grow on glycerol plates and on glucose plates containing HU (Figure 4, line 7).

Group 4 includes removal of succinylation/ubiquitination on Fum1 at K78/K79. K78 is conserved from yeast to human, while K79 is conserved from yeast to fish only, and an arginine can be found in the latter position in human (Supplementary Alignment 2). Accordingly, the effects of K78 mutations are much stronger than those of K79 with respect to DNA damage sensitivity. Fum1K78/K79 double mutant proteins are detected at much lower levels as compared to the wild-type Fum1 protein and this is true to a lower degree for the single mutations. This can explain the lower fumarase activity detected in these mutants. The most probable scenario, based on our data, is that modification of K78/K79 by succinylation/ubiquitination brings about degradation of fumarase, and upon DNA damage induction unmodified versions of the protein with high enzymatic activity are synthesized (see Graphical Abstract). It is also possible that Fum1 undergoes demodification, but we do not have direct proof for this. In the structure of yeast Fum1, Group 3 and 4 residues can be found in close proximity to the catalytic site (represented by H154, which forms an intermediate with fumarate; Figure 10(a)), with the exception of R239, which is located further away. Group 1 and 2 residues, on the other hand, are all located away from the catalytic site (Figure 10(b)).

Previous studies have shown that FH is recruited to the site of damaged DNA. Consistently, we find that recruitment of wild-type Fum1 to the cleaved *HO*-site increases approximately five-fold. Fum1 mutant proteins K78E/K79E (K789E), T122E, S124D, T126E, S128D, H154R and R239Q were not recruited to the cleaved *HO*-site. Notably, Fum1S128D mutant protein was not recruited to the site of DNA damage, suggesting that the mutation S128D in fumarase prevents the recruitment of fumarase to the site of DNA damage. However, the Fum1S128D was still able to support both TCA cycle and DNA repair, which suggests that the recruitment of Fum1 to the site of damaged DNA is not a requirement for its functional role in the DNA damage response. In this regard it has been shown that in both yeast and human cells deleted for the fumarase gene can be rescued upon DNA damage by the organic acid fumarate added to the growth medium.[5] In addition, yeast cells deleted for the fumarase gene can be rescued by expression of a bacterial homolog of fumarase.[24] Thus, together these data support the notion that recruitment of Fum1 to the damaged DNA is not an absolute requirement for its DNA repair related function.

Materials and Methods

Strains and plasmids

*BY*4741Δ*W* and *BY*4742Δ*W* and their gene deletion derivative strains were generated from parental strains obtained from EUROSCARF. *TRP1* knockout was achieved through insertion of *hisG* with the help of *NKY1009*.[25] *BY*4743Δ*W* and the gene deletion derivatives were generated by mating the respective *BY*4741Δ*W* and *BY*4742Δ*W* strains and plating on plates lacking both methionine and lysine. The consensus *HO*-site TTTTAGTTTCAGCTTTCCGCAACAGTATAATTT-TATAAACCC was inserted in between the *Nsi*I and *Xho*I sites of the plasmid *puc8+HIS3*.[26] The *HIS3* marker was used to knock the *HO*-site in between the *HIS3* and *DED1* loci on chromosome XV of *BY*4742Δ*W* and *BY*4742Δ*W*Δ*FUM1* by transforming those strains with *Bam*HI-cut *puc8+HIS3-HO42* and plating onto plates lacking histidine. Correct insertions were confirmed by DNA sequencing. A complete list of strains used in the study is listed

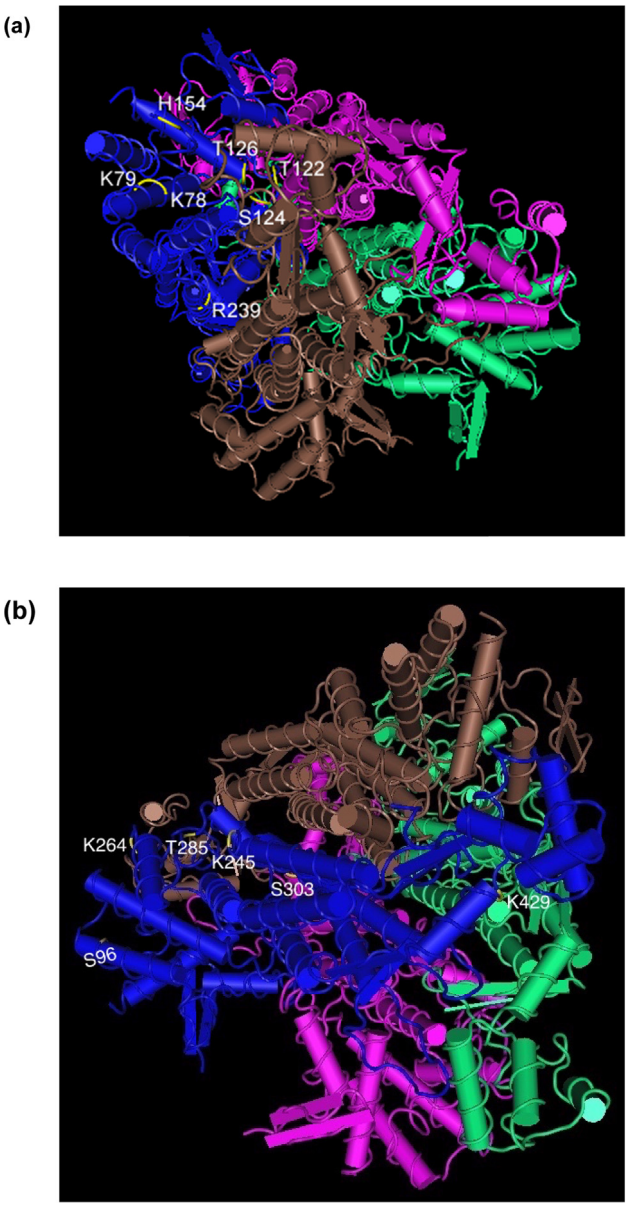

Figure 10. Location of the PTM sites in the structure of yeast Fum1 (Source: PDB ID: 1YFM). Fumarase is a tetrameric protein made of four identical subunits, each of which is represented by a different colour (blue, brown, green or magenta). (a) The residues that were identified to be modified through MS and had functional significance are shown in yellow on the backbone of the polypeptide, while the respective residues are indicated in white. They are seen to cluster around the catalytic site, which is where the residue H154 is located. The site R239 was seen to be located furthest away from the active site. (b) The residues that were identified to be modified through MS but had no functional significance are shown in yellow on the backbone of the polypeptide, while the respective residues are indicated in white. They are located away from the catalytic site.

in Supplementary Table 1. The TRP1-marked *HOT1* plasmid expressing the HO endonuclease under the control of the *GAL10* promoter has been described previously.[19] To facilitate cloning of the *FUM1* open reading frame (ORF), the internal *Eco*RI site was eliminated by sequential PCR. The plasmids *PactT424-HA-Fum*1Δ*MTS* and *PactT424-Fum*1Δ*MTS* that overexpress cytosolic fumarase from the strong *ACT1* promoter/terminator cassette were generated by cloning the *FUM*1Δ*MTS* PCR fragment *Eco*RI-*Sal*I into *PactT424* and *PactT424-HA*[27] which are based on the *TRP1*-marked multi-copy vector RS424.[28] *Pfum314-HA*$_3$-*H*$_{10}$-*Fum*1Δ*MTS* expresses cytosolic fumarase N-terminally tagged with three HA epitopes and ten histidines from its own promoter. It is based on the *TRP1*-marked single-copy plasmid *RS314*[28] and was generated by cloning the

*FUM*1Δ*MTS* PCR fragment *Eco*RI-*Sal*I into *PactT314-HA*$_3$-*H*$_{10}$ and replacing the *ACT1* promoter *Apa*I-*Nco*I with the *FUM1* promoter. *PactT316-HA-Fum*1Δ*MTS-myc9* expresses cytosolic fumarase N-terminally tagged with the HA epitope and C-terminally tagged with nine myc epitopes from the *ACT1* promoter. It is based on the *URA3*-marked single-copy plasmid *RS316*[28] and was generated by cloning the *FUM*1Δ*MTS* PCR fragment *Eco*RI-*Sal*I into *PactT316-HA-myc9*. *FUM1-HA*$_3$*H*$_{10}$*-33* was derived by cloning the *Eco*RI-*Sal*I *FUM1* PCR fragment with the *FUM1* promotor but without the stop codon into the *URA3*-marked single-copy plasmid *YCplac33*[29] that contained the HA$_3$-H$_{10}$ tag followed by the *ACT1* terminator. *FUM*1Δ*MTS-HA*$_3$*H*$_{10}$*-33* was constructed by first cloning the *FUM1* promoter *Not*I-*Eco*RI into *Pcup1-Cub-RUra314*[30] and the *FUM*1Δ*MTS* PCR fragment without stop codon *Eco*RI-*Sal*I into the resulting plasmid. Next, the *Sac*I-*Sal*I *FUM*1Δ*MTS* fragment including *FUM1* promoter but without the stop codon was cloned into the *URA3*-marked single-copy plasmid *YCplac33* that contained the HA$_3$-H$_{10}$ tag followed by the *ACT1* terminator. The mutations preventing or mimicking the observed PTMs were generated by sequential PCR with the primers listed in Supplementary Table 2.

Chromatin immunoprecipitation (ChIP) assay

Cells were cultured in dropout SD medium containing 2% raffinose weight volume (w/v) till A_{600nm} reached 1. Endonuclease expression was induced by resuspending cells in SD medium containing 2% (w/v) galactose and incubating them with shaking at 200 rotations per minute (rpm) at 28 °C for two hours. Chromatin crosslinking was performed with 1% formaldehyde for 20 min at 28 °C with gentle agitation and stopped with 150 mM glycine for five minutes. Yeast cells were harvested, resuspended in 0.5 ml 100 mM Tris buffer, pH 9, with 10 mM DTT and 12 μl of 0.1 g zymolyase dissolved in 1.6 ml of 10% Sorbitol and incubated at 30 °C for 30 min. 0.5 ml of 2× yeast lysis buffer (YLB) [200 mM Tris/HCl (pH 7.4), 100 mM KCl, 2 mM EDTA and 0.2% Nonidet P40], 2 mM PMSF and acid-washed glass beads were added. Cells were broken using a Mini beadbeater (Bertin Instruments) three times for 1 min at 6,000 rpm. Yeast lysates were collected and centrifuged in a microcentrifuge at 4 °C at 15,871**g** for 30 min. Pellets were resuspended in 500 μl of 1× YLB and sonicated. Sonication was performed using a cup-horn sonicator at 65% maximal amplitude for 30 s for a total of ten times. Sonicates were centrifuged in a microcentrifuge at 4 °C at 15,871**g** for 15 min and the supernatant transferred to new microfuge tubes. De-crosslinking of input was accomplished by adding 150 μl of pronase working buffer [100 mM Tris/HCl (pH 7.4), 0.5% SDS] and 10 μl of 20 μg/μl pronase (Roche). The mixture was incubated at 42 °C for two hours and 65 °C for six hours. DNA was extracted with 5:1 phenol/chloroform (Bio-Rad) and precipitated with ethanol. 20 μl bed volume of anti-HA antibody-coupled agarose beads (Thermo Fisher) were used for every 100 μl of chromatin solution for immunoprecipitation. Three washes using 1 ml YLB were performed and after the final wash, buffer volume equivalent to twice the bead bed volume was added to the tube. In addition, fish sperm DNA [75 ng/μl] and BSA [0.1 μg/μl] were added. The beads were incubated at 4 °C with rotation for 30 min. The beads were then washed two times with 1 ml of YLB before chromatin solution was added. The tubes were incubated overnight at 4 °C with rotation. The following day, the beads were washed ten times at 4 °C with rotation in the following sequence: three times for ten minutes each with 1 ml YLB, three times for ten minutes each with 1 ml YLB with 0.5 M NaCl, three times for 15 min each with 1 ml ChIP wash buffer [100 mM Tris/HCl (pH 7.4), 0.25 M LiCl, 0.5% Nonidet P40 and 0.5% sodium deoxycholate] and one time for 15 min with 1 ml TE buffer [10 mM Tris/HCl (pH 7.5) + 1 mM EDTA]. Chromatin bound to the beads was eluted by adding 110 μl of ChIP elution buffer [50 mM Tris/HCl (pH 7.4), 10 mM EDTA and 1% SDS] to each sample and heating them to 65 °C for ten minutes. The samples were then centrifuged at 1150**g** for one minute and the supernatant was transferred to new microfuge tubes. De-crosslinking of the eluate was accomplished by adding 100 μl of TE buffer and 10 μl of 20 μg/μl pronase to the supernatant. The mixture was incubated at 42 °C for two hours and 65 °C for six hours following which DNA purification was performed as described earlier. Real-time quantitative PCR was performed using SYBR Green PCR Master Mix (Applied Biosystems) with the chromatin isolated. Primers flanking the endonuclease site were: 5His3stp60 CCACCAAAGGTGTTCTTATGTAG and 3HO42nsi60 CGGAAAGCTGAAACTAAAATGCAT. The amplicon size was 160 bp. Real-time PCR was performed in quadruplicate and the Ct values obtained for the precipitated samples were normalized to the Ct values of their input. The data are shown as Mean ± S.D with the error bars indicating the S.D. All statistical calculations and graphs were computed in MS Excel.

Enzyme activity assay

Yeast cells expressing fumarase were inoculated in 50 ml SD medium containing 2% glucose and grown at 28 °C till A_{600nm} reached 1. Cells where DNA damage was induced were grown till A_{600nm} reached 0.8. These cells were harvested through centrifugation and resuspended in SD medium with 2% glucose containing 400 mM HU for 2 h. Cells were collected and resuspended in 1 ml YLB. Cell lysis was carried out by bead beating

followed by sonication as per parameters are described in the previous section. Total protein concentration was determined by NanoDrop (Thermo Scientific). Malate dehydrogenase-coupled enzyme assay described elsewhere[11] was used to measure the specific activity of fumarase and its PTM mutants.

Cycloheximide chase assay

S. cerevisiae cells were grown in SD media containing 2% glucose to A_{600nm} = 1. Cycloheximide (200 mg/l) was added to half of the cultures, while HU (400 mM) and cycloheximide (200 mg/l) was added to the second half of the cultures. Aliquots were taken every hour for three hours, and equal amount of cells were analyzed by Western Blot with primary antibodies against fumarase,[5] HA (Roche) or myc (Roche), followed by staining with a horseradish peroxidase-coupled secondary anti-rabbit (fumarase) or anti-mouse (HA and myc) IgG antibody. Coomassie Brilliant Blue (Sigma) staining with equal amounts of cells loaded onto a separate gel served as loading control. The intensities of the bands were quantified with a BioRad ChemiDoc XRS. The ratio of the band intensities before the addition of cycloheximide (time = 0) was set as 1, and the error bars represent the deviations between duplicates. Representative Western blots are shown. The half-life of fumarase was calculated using trendline (excel).

Mass spectrometry

Protein bands corresponding to the size of tagged Fum1 were excised from the polyacrylamide gel stained with Coomassie Blue and in-gel trypsinated. The tryptic peptides were subjected to liquid chromatography–mass spectrometry (LC–MS) analysis using an Eksigent nanoIC Ultra and ChiPLC-nanoflex (Eksigent) in trap-elute configuration, with a 200 μm × 0.5 mm trap column and a 75 μm × 150 mm analytical column. Both trap and analytical columns were made of ChromXP C18-CL, 3 μm (Eksigent). Peptides were separated by a gradient formed by 2% ACN, 0.1% FA (mobile phase A) and 98% ACN, 0.1% FA (mobile phase B): 5–7% of mobile phase B in 0.1 min, 7–30% of mobile phase B in 10 min, 30–60% of mobile phase B in 4 min, 60–90% of mobile phase B in 1 min, 90–90% of mobile phase B in 5 min, 90–5% of mobile phase B in 1 min and 5–5% of mobile phase B in 10 min, at a flow rate of 300 nl/min. The MS analysis was performed on a TripleTOF 5600 system (AB SCIEX, Foster City, CA, USA) in Information Dependent Mode. MS spectra were acquired across the mass range of 400–1250 *m/z* in high resolution mode (>30,000) using 250 ms accumulation time per spectrum. A maximum of 10 precursors per cycle were chosen for fragmentation from each MS spectrum with 100 ms minimum accumulation time for each precursor and dynamic exclusion for 8 s. Tandem mass spectra were recorded in high sensitivity mode (resolution >15,000) with rolling collision energy on. Peptide identification and the detection of post-translational modifications were carried out with the ProteinPilot 5.0 software Revision 4769 (AB SCIEX) using the Paragon database search algorithm (5.0.0.0.4767), against a protein sequence database (6723 entries) of the yeast *S. cerevisiae*.

Acknowledgements

We thank Ms Yardena Silas, Ms Rachel Teo, Ms Si Min Lang and Ms Chia Lynn Choo for critical comments on the manuscript and students from Clementi Town Secondary School for practical support. This work was supported by grants from the National Research Foundation (NRF) to OP and NL.

Author contributions

SW produced Figures S2–S6; DR repeated the experiments, produced Figure S7 and wrote part of the manuscript; JT produced Figures 5 and S1; JL repeated the experiments; JY and AC supported SW; ZY supported the MS experiments; TKL performed the MS experiments; QL supervised TKL; OP co-supervised SW, DR, LJ and ZY; NL supervised SW, DR, JT, JL, JY, AC, ZY and wrote the manuscript.

Declaration of Competing Interest

The authors declare that they have no known competing financial interests or personal relationships that could have appeared to influence the work reported in this paper.

Appendix A. Supplementary material

Supplementary data to this article can be found online at https://doi.org/10.1016/j.jmb.2020.09.021.

Received 18 May 2020;
Accepted 27 September 2020;
Available online 12 October 2020

Keywords:
Fumarase;
post-translational modification;
enzymatic activity;
DNA repair;
TCA cycle

† The first two authors contributed equally to the work.

Abbreviations used: 2SC, S-(2-succinyl) cysteine; 22, YCplac22; 33, YCplac33; AMPK, AMP-activated protein kinase; bp, base pairs; DNA-PK, DNA-dependent protein kinase; DNA-PKcs, DNA-PK catalytic subunit; DSB, double-strand break; EMT, epithelial-to-mesenchymal-transition; FH, fumarate hydratase; FOXM1, forkhead box protein M1; Fum1, fumarase; HA, hemagglutinin; HIF, hypoxia-inducible factor; HLRCC, hereditary leiomyomatosis and renal cell carcinoma; HOT1, TRP1-marked plasmid expressing the homothallic switching endonuclease under the control of the GAL10 promoter; HR, homologous recombination; HU, hydroxyurea; MS, mass spectrometry; MTS, mitochondrial targeting signal; NHEJ, non-homologous end joining; NRF2, nuclear factor (erythroid-derived 2)-like 2; ORF, open reading frame; PTM, post-translational modification; RCC, renal cell cancer; rpm, rotations per minute; SD, synthetic depleted; TCA, tricarboxylic acid; VEGF, vascular endothelial growth factor; w/v, weight volume; YLB, yeast lysis buffer

References

1. Yogev, O., Naamati, A., Pines, O., (2011). Fumarase: A paradigm of dual targeting and dual localized functions. *FEBS J.*, **278**, 4230–4242.
2. Dik, E., Naamati, A., Asraf, H., Lehming, N., Pines, O., (2016). Human fumarate hydratase is dual localized by an alternative transcription initiation mechanism. *Traffic*, **17**, 720–732.
3. Leshets, M., Ramamurthy, D., Lisby, M., Lehming, N., Pines, O., (2018). Fumarase is involved in DNA double-strand break resection through a functional interaction with Sae2. *Curr. Genet.*, **64**, 697–712.
4. Leshets, M., Silas, Y.B.H., Lehming, N., Pines, O., (2018). Fumarase: From the TCA cycle to DNA damage response and tumor suppression. *Front. Mol. Biosci.*, **25**, 68.
5. Yogev, O., Yogev, O., Singer, E., Shaulian, E., Goldberg, M., Fox, T.D., Pines, O., (2010). Fumarase: A mitochondrial metabolic enzyme and a cytosolic/nuclear component of the DNA damage response. *PLoS Biol.*, **8**, e1000328.
6. Jiang, Y., Qian, X., Shen, J., Wang, Y., Li, X., Liu, R., Xia, Y., Chen, Q., et al., (2015). Local generation of fumarate promotes DNA repair through inhibition of histone H3 demethylation. *Nat. Cell Biol.*, **17**, 1158–1168.
7. Sulkowski, P.L., Sundaram, R.K., Oeck, S., Corso, C.D., Liu, Y., Noorbakhsh, S., Niger, M., Boeke, M., et al., (2018). Krebs-cycle-deficient hereditary cancer syndromes are defined by defects in homologous-recombination DNA repair. *Nat. Genet.*, **50**, 1086–1092.
8. Reed, W.B., Walker, R., Horowitz, R., (1973). Cutaneous leiomyomata with uterine leiomyomata. *Acta Derm. Venereol.*, **53**, 409–416.
9. Launonen, V., Vierimaa, O., Kiuru, M., Isola, J., Roth, S., Pukkala, E., Sistonen, P., Herva, R., et al., (2001). Inherited susceptibility to uterine leiomyomas and renal cell cancer. *Proc. Natl. Acad. Sci. U. S. A.*, **98**, 3387–3392.
10. Alam, N.A., Bevan, S., Churchman, M., Barclay, E., Barker, K., Jaeger, E.E., Nelson, H.M., Healy, E., et al., (2001). Localization of a gene (MCUL1) for multiple cutaneous leiomyomata and uterine fibroids to chromosome 1q42.3-q43. *Am. J. Hum. Genet.*, **68**, 1264–1269.
11. Tomlinson, I.P., Alam, N.A., Rowan, A.J., Barclay, E., Jaeger, E.E., Kelsell, D., Leigh, I., Gorman, P., et al., (2002). Germline mutations in FH predispose to dominantly inherited uterine fibroids, skin leiomyomata and papillary renal cell cancer. *Nat. Genet.*, **30**, 406–410.
12. Wang, T., Yu, Q., Li, J., Hu, B., Zhao, Q., Ma, C., Huang, W., Zhuo, L., et al., (2017). O-GlcNAcylation of fumarase maintains tumour growth under glucose deficiency. *Nat. Cell. Biol.*, **19**, 833–843.
13. Henriksen, P., Wagner, S.A., Weinert, B.T., Sharma, S., Bacinskaja, G., Rehman, M., Juffer, A.H., Walther, T.C., et al., (2012). Proteome-wide analysis of lysine acetylation suggests its broad regulatory scope in Saccharomyces cerevisiae. *Mol. Cell. Proteom.*, **11**, 1510–1522.
14. Weinert, B.T., Scholz, C., Wagner, S.A., Iesmantavicius, V., Su, D., Daniel, J.A., Choudhary, C., (2013). Lysine succinylation is a frequently occurring modification in prokaryotes and eukaryotes and extensively overlaps with acetylation. *Cell Rep.*, **4**, 842–851.
15. Reinders, J., Wagner, K., Zahedi, R.P., Stojanovski, D., Eyrich, B., van der Laan, M., Rehling, P., Sickmann, A., et al., (2007). Profiling phosphoproteins of yeast mitochondria reveals a role of phosphorylation in assembly of the ATP synthase. *Mol. Cell. Proteom.*, **6**, 1896–1906.
16. Swaney, D.L., Beltrao, P., Starita, L., Guo, A., Rush, J., Fields, S., Krogan, N.J., Villén, J., (2013). Global analysis of phosphorylation and ubiquitylation cross-talk in protein degradation. *Nat. Methods*, **10**, 676–682.
17. Ray, B.L., White, C.I., Haber, J.E., (1991). Heteroduplex formation and mismatch repair of the “stuck” mutation during mating-type switching in Saccharomyces cerevisiae. *Mol. Cell. Biol.*, **11**, 5372–5380.
18. Meiron, H., Nahon, E., Raveh, D., (1995). Identification of the heterothallic mutation in HO-endonuclease of *S. cerevisiae* using HO/ho chimeric genes. *Curr. Genet.*, **28**, 367–373.
19. Jensen, R.E., Herskowitz, I., (1984). Directionality and regulation of cassette substitution in yeast. *Cold Spring Harbor Symp. Quant. Biol.*, **49**, 97–104.
20. Jackson, S.P., Bartek, J., (2009). The DNA-damage response in human biology and disease. *Nature*, **461**, 1071–1078.
21. Khanna, K.K., Jackson, S.P., (2001). DNA double-strand breaks: signaling, repair and the cancer connection. *Nat. Genet.*, **27**, 247–254.
22. Wright, W.D., Shah, S.S., Heyer, W.D., (2018). Homologous recombination and the repair of DNA double-strand breaks. *J. Biol. Chem.*, **293**, 10524–10535.
23. Scully, R., Panday, A., Elango, R., Willis, N.A., (2019). DNA double-strand break repair-pathway choice in somatic mammalian cells. *Nat. Rev. Mol. Cell Biol.*, **20**, 698–714.
24. Singer, E., Silas, Y.B., Ben-Yehuda, S., Pines, O., (2017). Bacterial fumarase and L-malic acid are evolutionary ancient components of the DNA damage response. *Elife*, **6** pii: e30927.
25. Alani, E., Cao, L., Kleckner, N., (1987). A method for gene disruption that allows repeated use of URA3 selection in the construction of multiply disrupted yeast strains. *Genetics*, **116**, 541–545.
26. Chew, B.S., Siew, W.L., Xiao, B., Lehming, N., (2010). Transcriptional activation requires protection of the TATA-binding protein Tbp1 by the ubiquitin-specific protease Ubp3. *Biochem. J.*, **431**, 391–399.

27. Lim, M.K., Siew, W.L., Zhao, J., Tay, Y.C., Ang, E., Lehming, N., (2011). Galactose induction of the GAL1 gene requires conditional degradation of the Mig2 repressor. *Biochem. J.*, **435**, 641–649.
28. Sikorski, R.S., Hieter, P., (1989). A system of shuttle vectors and yeast host strains designed for efficient manipulation of DNA in Saccharomyces cerevisiae. *Genetics*, **122**, 19–27.
29. Gietz, R.D., Sugino, A., (1988). New yeast-*Escherichia coli* shuttle vectors constructed with in vitro mutagenized yeast genes lacking six-base pair restriction sites. *Gene*, **74**, 527–534.
30. Laser, H., Bongards, C., Schäller, J., Heck, S., Johnsson, N., Lehming, N., (2000). *Proc. Natl. Acad. Sci. U. S. A.*, **97**, 13732–13737.